







ORIGINAL RESEARCH

Significant Delayed Activation on the Right Ventricular Outflow Tract Represents Complete Right Bundle-Branch Block Pattern in Brugada Syndrome

Yoshimasa Morimoto , MD; Hiroshi Morita , MD, PhD; Kentaro Ejiri , MD, PhD; Tomofumi Mizuno , MD; Takuro Masuda, MD; Akira Ueoka, MD, PhD; Saori Asada, MD, PhD; Masakazu Miyamoto, MD; Satoshi Kawada, MD, PhD; Koji Nakagawa, MD, PhD; Nobuhiro Nishii , MD, PhD; Kazufumi Nakamura , MD, PhD; Hiroshi Ito, MD, PhD

BACKGROUND: The appearance of complete right bundle-branch block (CRBBB) in Brugada syndrome (BrS) is associated with an increased risk of ventricular fibrillation. The pathophysiological mechanism of CRBBB in patients with BrS has not been well established. We aimed to clarify the significance of a conduction delay zone associated with arrhythmias on CRBBB using body surface mapping in patients with BrS.

METHODS AND RESULTS: Body surface mapping was recorded in 11 patients with BrS and 8 control patients both with CRBBB. CRBBB in control patients was transiently exhibited by unintentional catheter manipulation (proximal RBBB). Ventricular activation time maps were constructed for both of the groups. We divided the anterior chest into 4 areas (inferolateral right ventricle [RV], RV outflow tract [RVOT], intraventricular septum, and left ventricle) and compared activation patterns between the 2 groups. Excitation propagated to the RV from the left ventricle through the intraventricular septum with activation delay in the entire RV in the control group (proximal RBBB pattern). In 7 patients with BrS, excitation propagated from the inferolateral RV to the RVOT with significant regional activation delay. The remaining 4 patients with BrS showed a proximal RBBB pattern with the RVOT activation delay. The ventricular activation time in the inferolateral RV was significantly shorter in patients with BrS without a proximal RBBB pattern than in control patients.

CONCLUSIONS: The CRBBB morphology in patients with BrS consisted of 2 mechanisms: (1) significantly delayed conduction in the RVOT and (2) proximal RBBB with RVOT conduction delay. Significant RVOT conduction delay without proximal RBBB resulted in CRBBB morphology in patients with BrS.

Key Words: activation pattern ■ body surface map ■ Brugada syndrome ■ complete right bundle-branch block

Brugada syndrome (BrS) is characterized by coved-type ST elevation in the right precordial leads and sudden cardiac death caused by nocturnal ventricular fibrillation (VF).¹ Although the mechanisms underlying the ECG changes and VF remain controversial, repolarization abnormality and/or depolarization abnormality have been critical

in the pathogenesis of BrS.^{2–6} In recent years, the epicardial ablation technique has revealed conduction abnormality on the epicardial surface of the right ventricular free wall, particularly the right ventricular outflow tract (RVOT).^{7,8} Abnormal delayed activation of the RVOT could be a source of ST elevation and a substrate of VF in patients with BrS.⁹

Correspondence to: Hiroshi Morita, MD, PhD, Department of Cardiovascular Therapeutics, Okayama University Graduate School of Medicine, Dentistry, and Pharmaceutical Sciences, 2-5-1 Shikata-cho, Kita-ku, Okayama 700-8558, Japan. Email: hmorita@cc.okayama-u.ac.jp

This manuscript was sent to Barry London, MD, PhD, Senior Guest Editor, for review by expert referees, editorial decision, and final disposition.

Supplemental Material is available at <https://www.ahajournals.org/doi/suppl/10.1161/JAHA.122.028706>

For Sources of Funding and Disclosures, see page 15.

© 2023 The Authors. Published on behalf of the American Heart Association, Inc., by Wiley. This is an open access article under the terms of the [Creative Commons Attribution-NonCommercial-NoDerivs](#) License, which permits use and distribution in any medium, provided the original work is properly cited, the use is non-commercial and no modifications or adaptations are made.

JAHA is available at: www.ahajournals.org/journal/jaha

CLINICAL PERSPECTIVE

What Is New?

- Body surface mapping showed a significant conduction delay around the right ventricular outflow tract in patients with BrS with complete right bundle-branch block (CRBBB) and a different right ventricle activation pattern in these patients than that in patients with CRBBB due to conduction block at the proximal right bundle branch.
- Extended depolarization abnormality on the epicardium around the right ventricular outflow tract might exhibit CRBBB morphology in patients with BrS, being consistent with the worse outcome in patients with BrS with CRBBB.

What Are the Clinical Implications?

- This observation might provide insights into the diagnosis of BrS masked by CRBBB, although further study would be needed.

Nonstandard Abbreviations and Acronyms

BrS	Brugada syndrome
BSM	body surface mapping
CRBBB	complete right bundle-branch block
RBB	right bundle branch
VAT	ventricular activation time

Complete right bundle-branch block (CRBBB) can occur in patients with BrS. Previous studies have shown that patients with BrS with CRBBB might have a severe clinical phenotype, such as frequent VF episodes or electrical storm.¹⁰ CRBBB usually occurs due to a complete conduction block at the main trunk of the right bundle branch (RBB), and activation of the right ventricle (RV) originates from the left ventricle (LV) through the intraventricular septum.¹¹

Recently, it has been reported that the conduction block at the trunk of the left bundle branch usually causes left bundle-branch block; however, some patients have left bundle-branch block pattern with intact His-Purkinje conduction due to conduction disturbance being distant from the Purkinje system.^{12,13} Evaluation of the disturbed site could be useful for predicting the effects of His or left bundle-branch block pacing in patients with heart failure. The results of a study in which the block site of RBBB was evaluated were reported in the 1960s, which showed that RBBB was mainly present in the RBB trunk in various heart diseases.¹⁴ A study of patients with congenital heart

disease and who received surgical repairs showed that CRBBB could occur due to conduction blocks of the main trunk of the RBB, distal portion of the RBB, and conduction disturbance in the distal RV myocardium.¹⁵ However, the mechanism of CRBBB in BrS has not been well understood.

We hypothesized that delayed RV activation could contribute to the formation of the CRBBB pattern in patients with BrS who have significantly delayed activation of the RV free wall. The RV activation pattern in patients with BrS and CRBBB should be different from patients with “usual” CRBBB due to block of the main trunk of the RBB. The objective of this study was to clarify the significance of a conduction delay zone associated with arrhythmias in patients with BrS on the formation of CRBBB patterns using an 87-lead body surface mapping (BSM) system.

METHODS

Study Subjects

All data and supporting materials have been provided with the published article. This was a retrospective and observational study conducted at Okayama University Hospital, Okayama, Japan. The BrS group consisted of 11 patients with BrS with CRBBB. BrS diagnosis was made according to the Heart Rhythm Society/European Heart Rythm Association/Asian Pacific Heart Rhythm Society (HRS/EHRA/APHRS) expert consensus statement.¹ The J point was determined as the end point of the QRS interval in lead V5. The definition of CRBBB was based on American Heart Association/American College of Cardiology Foundation/Heart Rhythm Society (AHA/ACCF/HRS) recommendations for standard intercostal leads¹⁶: (1) QRS interval ≥ 120 ms, (2) rsR' or rSR' pattern in leads V1 and V2, and (3) S wave of greater duration R wave or >40 ms in leads I and V6. The control group consisted of 8 patients who did not have organic heart diseases and in whom it was confirmed that CRBBB was exhibited by transient RBB conduction disturbance by unintentional catheter manipulation around the RV septum during electrophysiological study (EPS) and/or ablation for any arrhythmias other than BrS. These CRBBBs resulted from direct conduction disturbances of the RBB truncus and were considered to be “usual CRBBBs.” All conduction disturbances improved within 5 minutes after the occurrence of CRBBB. To evaluate whether the activation pattern in control patients was considered as “usual CRBBB,” we also analyzed 5 patients with CRBBB without obvious heart disease. We collected the baseline clinical characteristics included age, sex, history of syncope or spontaneous VF, and family history of sudden death via medical chart. In the BrS group, we also evaluated

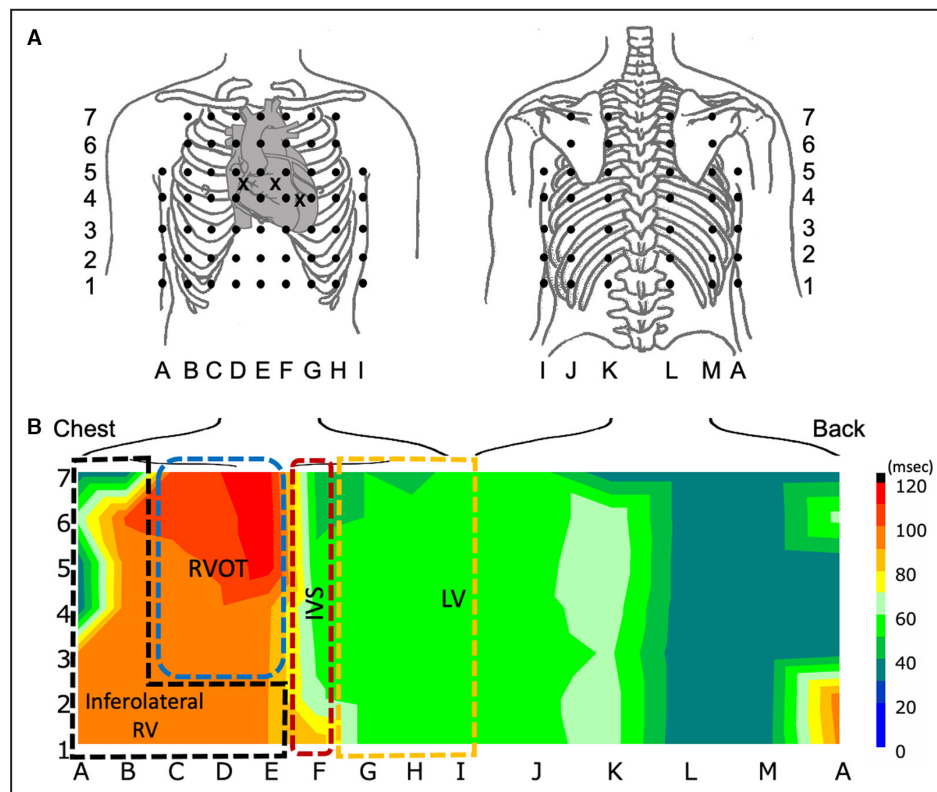


Figure 1. Body surface mapping system and interpretation of the body surface locations and divided areas of the ventricles.

A, Locations of electrodes in the 87-lead body surface mapping system (BSM). A–I are placed on the anterior chest, and J–M are located on the back. E is located at the median line of the anterior chest. A and I are located at the right and left midaxillary lines, respectively. Row 6 is placed at the level of the parasternal second intercostal space, and row 4 is placed at the midclavicular 5th intercostal space. Row 5 is placed between rows 6 and 4, and rows 7, 3, 2, and 1 are located vertically at equal intervals. Leads V1–V3 are positioned at crosses (X), and leads V4–6 are coincident with G4, H4, and I4, respectively. Adapted from Morita et al¹⁷ with permission. Copyright © 2008, Heart Rhythm Society. **B**, Isochronal map of ventricular activation time based on BSM (control group Case 5). Color bar at the right side of the map shows activation time from the onset of the QRS complex. Blue color shows an early activation area, and red color shows a late activation area. For statistical analysis, we divided the anterior 59 leads into 4 regions (inferior and lateral RV [A1–5, B1–7, C1–2, D1–2, E1–2], RVOT and mid RV [C3–7, D3–7, E3–7], septum [F1–7], and LV [G1–7, H1–7, I1–5]). Black dot square shows inferolateral RV, blue dot square shows RVOT and mild RV, brown dot square shows intraventricular septum, and yellow dot square shows LV. IVS indicates intraventricular septum; LV, left ventricle; RV, right ventricle; and RVOT, right ventricular outflow tract.

late potential using signal-averaged electrocardiography, 12-lead electrocardiography markers, VF induction by programmed electrical stimulation, and *SCN5A* mutation. *SCN5A* mutations were analyzed as we reported previously.¹⁷

All the patients provided written informed consent to participate in the study. This study complied with the Declaration of Helsinki and was approved by the Ethics Committee on Human Research and Epidemiology of Okayama University. *SCN5A* gene analysis was performed in 8 patients in compliance with the guidelines for human genome studies of the Ethics Committee of Okayama University.

Definition of Fragmented QRS, Late Potential, aVR Sign, S Wave in Lead I, and QTc Interval

We evaluated the signs of conduction disturbances by 12-lead ECG. A standard 12-lead ECG was recorded during sinus rhythm at 0 to 150 Hz for each patient.¹⁸ The QRS interval was measured for lead II. Based on the previous study, the presence of fragmented QRS for a wide QRS complex was defined as a QRS complex with >2 positive spikes within the QRS complex in 2 contiguous leads.¹⁹ A late potential by signal-averaged ECG was considered positive when 2 criteria

Table 1. Patient Characteristics

	Sex	Age (y)	Symptom/ arrhythmia	EPS	FH of SD	Spontaneous type-1	QRS interval (ms)	aVR sign [*]	S wave in lead I [†]	LP [‡]	HV Interval (ms)	SCN5A mutation	Induced VF by PES	QTc interval [§] (ms)	RV activation pattern with the proximal RBBB pattern
BrS group (BrS patients with CRBBB)															
1	M	50	VF	+	-	+	140	-	+	+	38	-	+	418	-
2	M	55	VF	+	+	+	158	+	+	+	43	-	+	456	-
3	M	73	VF	+	-	+	148	+	+	+	40	+	-	351	-
4	M	29	Syncope	+	+	+	170	+	+	+	50	+	-	472	-
5	M	43	None	+	+	+	168	-	+	+	52	-	-	421	-
6	M	62	Syncope	+	+	+	134	-	+	+	47	+	+	413	-
7	M	58	None	-	-	+	148	-	+	+	N/A	N/A	N/A	413	-
8	M	64	VF	+	-	+	146	-	+	+	39	-	+	374	+
9	M	47	VF	+	-	+	140	-	+	-	40	-	+	364	+
10	M	66	Syncope	-	-	+	170	+	+	+	N/A	N/A	N/A	479	+
11	M	61	None	-	-	+	144	-	+	+	N/A	N/A	N/A	387	+
Control group (patients with CRBBB)															
1	F	48	PVCs	+	-	-	130	-	+	-	37	N/A	-	438	+
2	F	34	PVCs	+	-	-	122	-	+	-	35	N/A	-	432	+
3	M	17	PVCs	+	-	-	144	+	+	-	39	N/A	-	462	+
4	M	36	PVCs	+	-	-	148	-	+	-	32	N/A	-	449	+
5	M	56	PVCs	+	-	-	136	-	+	-	35	-	-	377	+
6	M	52	AFL	+	-	-	128	-	+	N/A	46	N/A	N/A	423	+
7	F	60	AT	+	-	-	136	-	+	N/A	42	N/A	N/A	428	+
8	M	52	Syncope	+	-	-	128	-	+	-	45	-	-	414	+

AFL indicates atrial flutter; AT, atrial tachycardia; BrS, Brugada syndrome; CRBBB, complete right bundle-branch block; EPS, electrophysiological study; FH, family history; LP, late potential; N/A, not available; PES, programmed electrical stimulation; PVC, premature ventricular contraction; RBBB, right bundle-branch block; SD, sudden death; and VF, ventricular fibrillation.

^{*}aVR sign and S wave in lead I was evaluated under CRBBB condition.

[†]LP in the control group was the value before CRBBB condition.

[‡]QTc interval was measured from the 12-lead ECG.

($RMS_{40} < 20 \mu V$ and $LAS_{40} < 38 ms$) were met.²⁰ A positive aVR sign was defined as R wave $\geq 0.3 mV$ or R/q ratio ≥ 0.75 in lead aVR.²¹ A large S wave in lead I was defined as positive when the S wave in lead I was $\geq 0.1 mV$ and/or 40 ms.²² The QT interval on 12-lead ECG was measured from the onset of the QRS complex to the end of the T-wave to evaluate repolarization abnormality. QT interval was corrected for heart rate (QTc, Bazett's formula).

EPS were performed on patients who provided written informed consent. The induction of ventricular arrhythmia was attempted without the use of antiarrhythmic drugs in patients with BrS. Programmed electrical stimulation was performed at the RV apex and RVOT using extra stimuli at 2 cycle lengths (600 and 400 ms) to induce polymorphic ventricular tachycardia or VF, which required cardioversion to terminate. The HV interval was measured during EPS.

Analysis of Body Surface Maps

We recorded BSM with 87-lead unipolar ECGs in patients in the BrS and control groups using the HPM-7100 mapping system (Fukuda Denshi Co, Japan).^{23,24} In the control group, we recorded the BSM of transient CRBBB in the catheter laboratory. ECG data (87 unipolar leads, regular limb leads, and leads V1-3) were recorded on a magnetic disk. Of these leads, 59 were located in the anterior region of the chest (A-I) and 28 were located on the back (J-M). These locations are the standards for the system (Figure 1). The unipolar leads on the mid-to-right chest are sensitive to electrical activity in the RV. Similarly, the leads on the high to

midchest are most sensitive to electrical activity in the RVOT, and the leads on the left chest-to-back reflected the LV potentials.

Two independent and experienced observers (Y.M. and H.M.) reviewed the BSM results for each patient. Local ventricular activation time (VAT) was defined as the interval between the onset of the QRS complex and the peak negative dV/dT of the QRS complex of each lead during sinus rhythm.²⁵ We then created isochronal maps of the VAT for each patient. We also colored these maps by the gradient of the VAT with blue showing an early activation area and red showing a late activation area. We evaluated the activation patterns in the control and BrS groups. We also calculated the average VAT of each lead in the BrS and control groups, and created isochronal maps (average VAT map) to evaluate the difference in the RV activation pattern between the 2 groups. If there was an area where the activation pattern was visually different, we divided the ventricles into subgroups and investigated whether there was a statistically significant difference in the VAT of the region of interest (Figure 1). We also measured the latest VAT in each region, which was the most delayed VAT measured across leads in a specific region. When the VAT map revealed 2 or more RV activation patterns in the BrS group, the VAT was evaluated similarly.

We reviewed the unipolar ECG on BSM in the area where the activation pattern was visually different between the control and BrS groups to evaluate the difference in the QRS morphology in these unipolar leads.

To evaluate the repolarization abnormality, the QT interval was measured from all 87 leads on BSM, and each

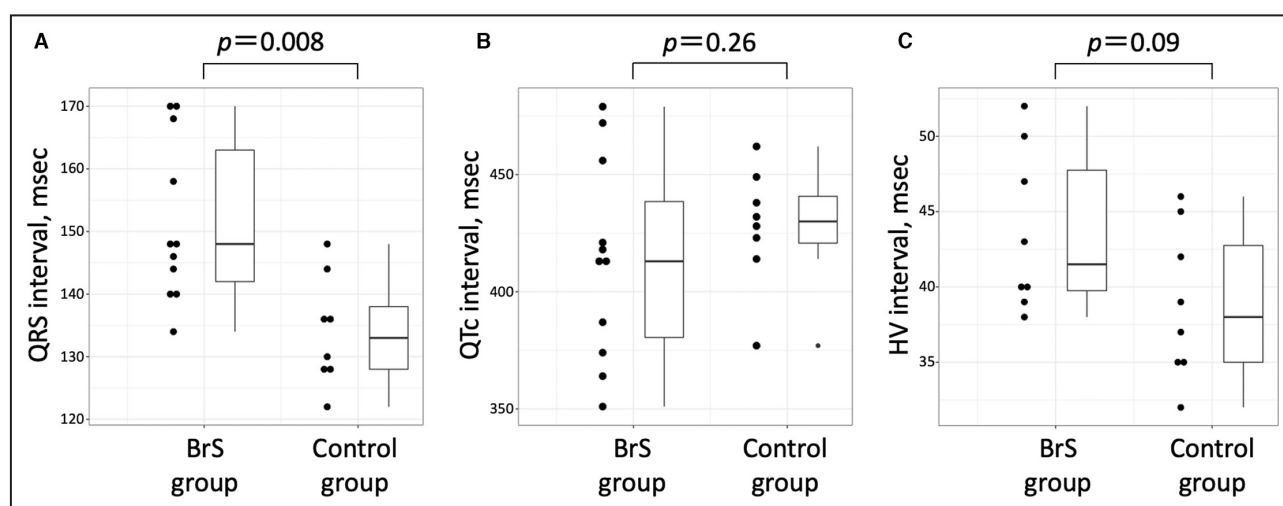


Figure 2. Comparison of the QRS interval, QTc interval on 12-lead ECG, and HV interval between the Brugada syndrome and the control groups.

QRS interval was significantly longer in the Brugada syndrome (BrS) group than that in the control group (A). There was no significant difference in QTc interval between the BrS group and the control group (B). HV interval tended to be longer in the BrS group than in the control group, but the difference was not significant (C).

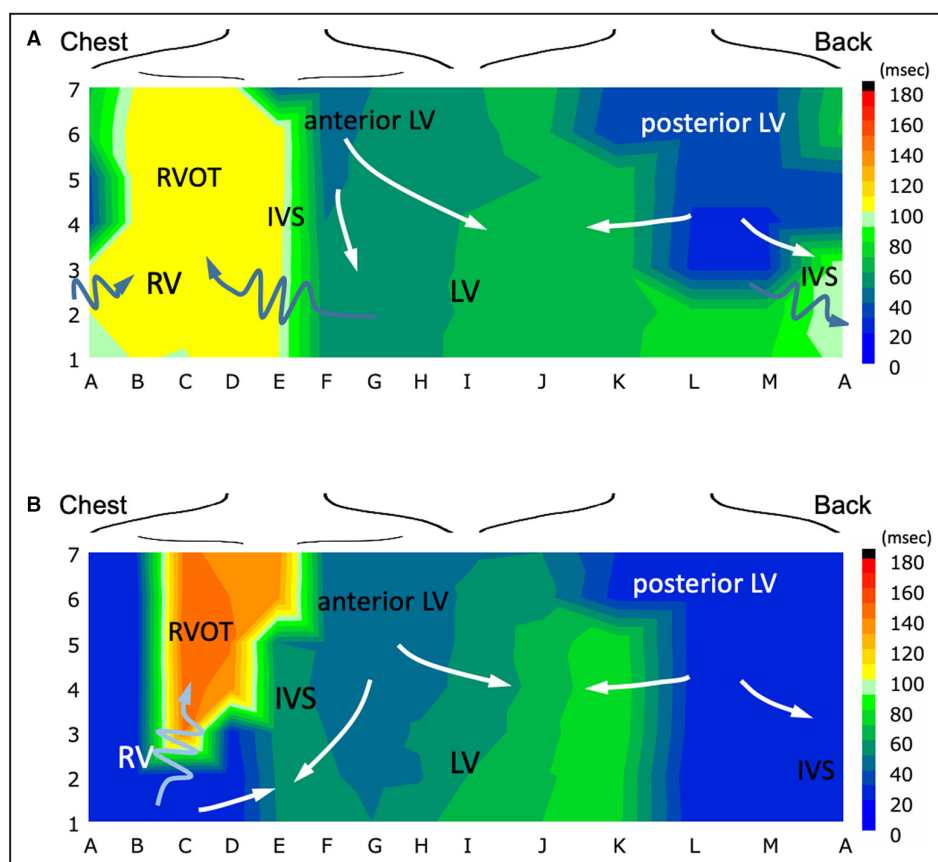


Figure 3. Interpretation of the ventricular activation time map.

A, The ventricular activation map of Case 1 in the control patients. Dark blue and green area represents early activation site. Yellow to orange area shows late activation site. Arrows show propagation of excitation, and zig-zag lines represent conduction delay. Excitation occurs from posterior left ventricle (LV) and anterior LV; those could represent excitations from posterior and anterior fascicles. Excitation propagated to right ventricle (RV) with conduction delay at the intraventricular septum. **B**, Ventricular activation map of Case 5 in the Brugada syndrome group. Excitations occur from LV and propagate to inferior site of RV, then propagated to RV outflow tract (RVOT) with significant conduction delay. IVS indicates intraventricular septum.

QTc interval was calculated (QTc, Bazett's formula). Then, we created isochronal maps of QTc interval in each patient and colored these maps by the gradient of the QTc interval with a blue color showing a shorter QTc interval area, and a red color showing a longer QTc interval area.¹⁷ We also created an average QTc interval map to compare the QTc heterogeneity between the 2 groups. We calculated the difference between the longest and shortest QTc intervals in the RVOT to evaluate QTc heterogeneity.

Statistical Analysis

First, we compared the baseline characteristics of the BrS and control groups. Continuous variables are presented as means with SDs. The QRS interval, QTc interval from 12-lead ECG, and HV interval during EPS were compared between the 2 groups using the Mann–Whitney *U* test.

To evaluate delayed conduction in the anterior surface of the RV, we statistically analyzed the VAT of only the chest leads. Fifty-nine leads were divided into 4 regions based on previous studies^{23,24}: inferior and lateral RV (A1-5, B1-7, C1-2, D1-2, E1-2; 18 leads), RVOT and mid RV (C3-7, D3-7, E3-7; 15 leads), septum (F1-7; 7 leads), and LV (G1-7, H1-7, I1-5; 19 leads) (Figure 1). For this analysis, we compared the log-transformed VAT stratified by the above 4 regions between the BrS and control groups using mixed-effect linear regression models with a compound symmetry correlation matrix taking into account within-participant correlation of each measure (as a per-lead analysis). The same analysis was applied for the comparison among subgroups according to different RV activation patterns in the BrS group.

To assess how different RV activation was delayed and where it was activated latest in the RV between

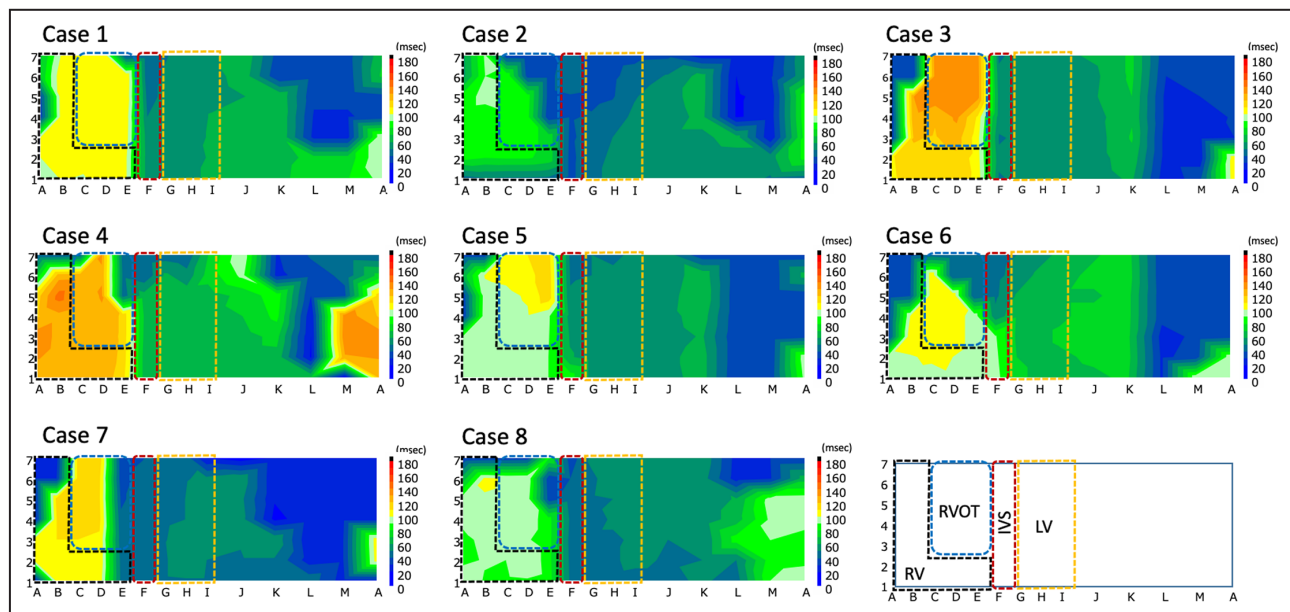


Figure 4. Ventricular activation time map in the control group.

Isochronal maps of ventricular activation time in control cases (Cases 1–8). Right ventricular (RV) activation occurred via transeptal spread toward the right ventricular outflow tract with delayed conduction in the entire RV in all patients. Black dot square shows inferolateral RV, blue dot square shows RVOT and mild RV, brown dot square shows intraventricular septum, and yellow dot square shows left ventricle. IVS indicates intraventricular septum; LV, left ventricle; and RVOT, right ventricular outflow tract.

the BrS and control groups, we compared the latest log-transformed VAT (the most delayed VAT across the leads) stratified by the above 4 region using Mann–Whitney *U* test (as a per-patient analysis).

Furthermore, we computed the difference between the longest and shortest QTc intervals among 15 leads in the RVOT and mid RV region, and then compared the differences between the BrS and control groups using Mann–Whitney *U* test (as a per-patient analysis). All comparisons and analyses were 2-tailed, and statistical significance was set at $P < 0.05$. All analyses were performed using R version 4.2.2 (The R Foundation for Statistical Computing, Vienna, Austria).

RESULTS

Patient Characteristics

The clinical characteristics of the 11 patients with BrS and 8 control patients are shown in Table 1. The reasons for EPS in patients in the control group were idiopathic premature ventricular contraction from the RVOT (Cases 1–5), atrial flutter (Case 6), paroxysmal atrial tachycardia (Case 7), and syncope (Case 8). In the BrS group, 5 patients experienced VF, 3 patients experienced syncope, and 3 patients were asymptomatic. Four patients (36%) had a family history of sudden death. Spontaneous type 1 ECG was observed in 10 patients (91%) and late potential was positive in 10 patients (91%). Fragmented QRS was observed in

all patients with BrS. Three of the 8 patients (27%) had *SCN5A* mutations. Eight patients (72%) underwent EPS, and VF was induced in 5 (63%) patients. The QRS interval was longer in the BrS group than that in the control group (151.5 ± 6.8 ms versus 134.0 ± 8.1 ms, $P = 0.008$, Figure 2A). The S-wave in lead I was observed in all patients in both groups. The aVR sign was observed in 4 patients (36%) in the BrS group and 1 patient (13%) in the control group. The QTc interval in the BrS group was not significantly different from the control group (413.5 ± 42.7 ms versus 427.9 ± 25.5 ms, $P = 0.26$, Figure 2B). The HV interval tended to be longer in the BrS group than in the control group, but the difference was not significant (43.6 ± 5.4 ms versus 38.9 ± 5.1 ms, $P = 0.09$, Figure 2C).

Difference in RV Activation Patterns

Figure 3 shows a typical VAT map of the control and BrS groups. The dark blue area represents the earliest activation site, followed by green, yellow, and red areas. The red area indicates a late activation site. Crowded color lines represent conduction delay area. Arrows indicate the propagation of excitation, and zig-zag lines represent conduction delays. The VAT map of Case 1 in the control group showed that excitation occurred from the posterior LV and anterior LV, which could represent excitations from the posterior and anterior fascicles, respectively. Excitation propagated to the RV with conduction delay at the intraventricular septum (Figure 3A). The VAT map of Case 5 in the

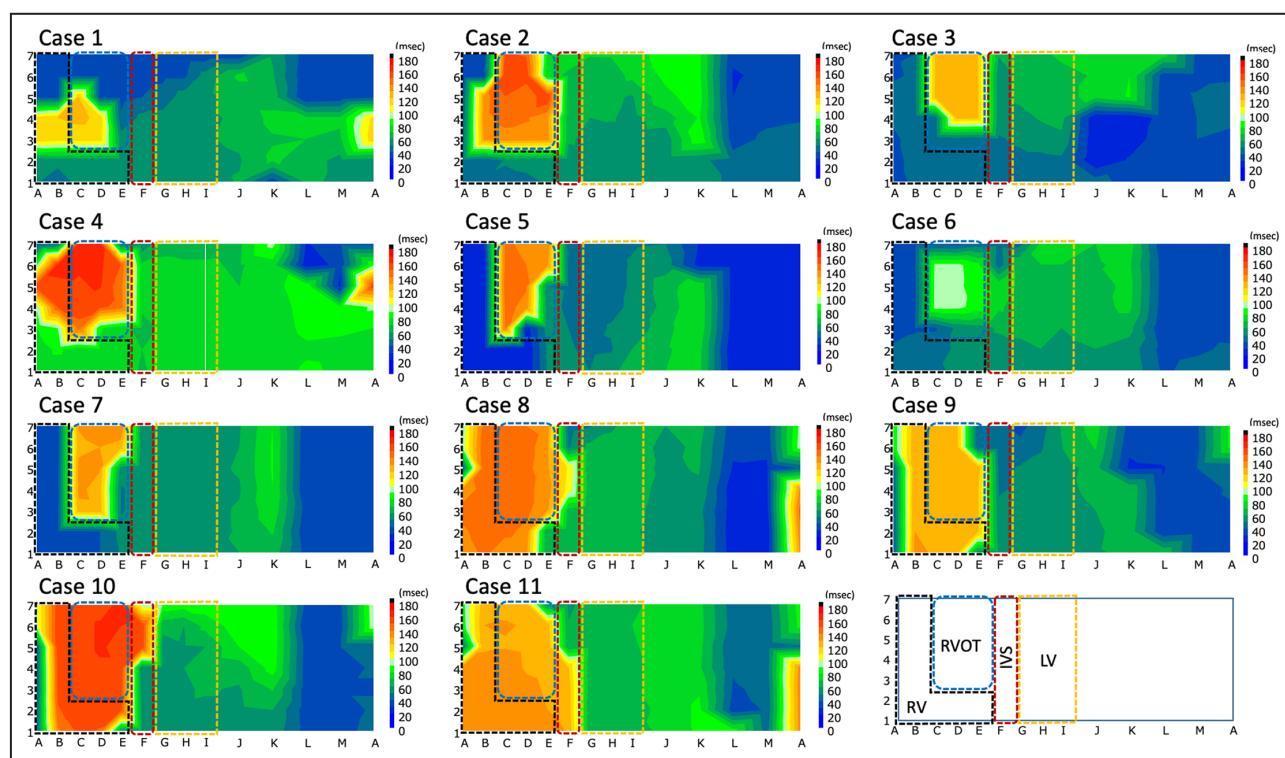


Figure 5. Ventricular activation time map in the Brugada syndrome group.

Isochronal maps of ventricular activation time in patients with Brugada syndrome (BrS) (Cases 1–11). There were 7 patients in the BrS group without the proximal right bundle-branch block pattern (Cases 1–7). The right ventricular (RV) activation propagated from the inferior and lateral RV toward the right ventricular outflow tract with significant activation delay. The other 4 patients (Cases 8–11) in the BrS group exhibited the RV activation pattern similar to that in the control group. Black dot square shows inferolateral RV, blue dot square shows RVOT and mild RV, brown dot square shows intraventricular septum, and yellow dot square shows left ventricle. IVS indicates intraventricular septum; LV, left ventricle; and RVOT, right ventricular outflow tract.

BrS group showed that excitations occurred from the LV, propagated to the inferior site of the RV, and then propagated to the RVOT with significant conduction delay (Figure 3B).

Figures 4 and 5 show all the VAT maps for the 2 groups. In the control group, all VAT maps showed that initial activation occurred in the LV area, and then ventricular activation propagated transseptally to the RV area and finally reached the RVOT. Activation of the entire RV area was delayed compared with that of the LV. This RV activation pattern indicates a proximal RBBB pattern. The ventricular activation pattern in patients with CRBBB without obvious heart disease was the same as that of the proximal RBBB pattern (Figure S1). In the BrS group, VAT maps indicated 2 RV activation patterns. In 7 patients in the BrS group (Cases 1–7), RV activation propagated from the inferior and lateral RV toward the RVOT. There was a significant conduction delay around the RVOT, whereas activation was not delayed in the inferior and lateral RV. This activation pattern was different from that of the proximal RBBB pattern. In the remaining 4 patients in the BrS group (Cases 8–11), after the initial LV activation, RV activation started from the intraventricular septum and

extended to the entire RV, and the activation pattern was similar to that in the control group. However, the entire RV showed more delayed conduction in patients in the BrS group than in the control group. Figure 6 shows the VAT maps according to the mean VAT for each patient. The VAT in the inferior and lateral RV was visually different overall in the BrS group, and the BrS group without the proximal RBBB pattern compared with that in the control group.

In the inferior and lateral RV where the VAT map was visually different, there was no significant difference in VAT between the overall BrS group and control group (76.4 ± 46.4 ms versus 89.1 ± 29.9 ms [4.15 ± 0.62 versus 4.41 ± 0.45 in log scale]; $P=0.20$, respectively). VAT at the inferior/lateral RV in the BrS group without the proximal RBBB pattern was significantly shorter than that in the control group (52.7 ± 30.3 ms versus 89.1 ± 29.9 ms [3.85 ± 0.46 versus 4.41 ± 0.45 in the log scale]; $P=0.003$), whereas VAT in other areas were not significantly different (Table 2, Figure 7). The latest VAT in the RVOT and mid RV in the BrS group was significantly longer than that in the control group (136.5 ± 23.2 ms versus 113.6 ± 15.6 ms [4.72 ± 0.14 versus 4.92 ± 0.16 in log scale]; $P=0.012$) (Table 3, Figure 8).

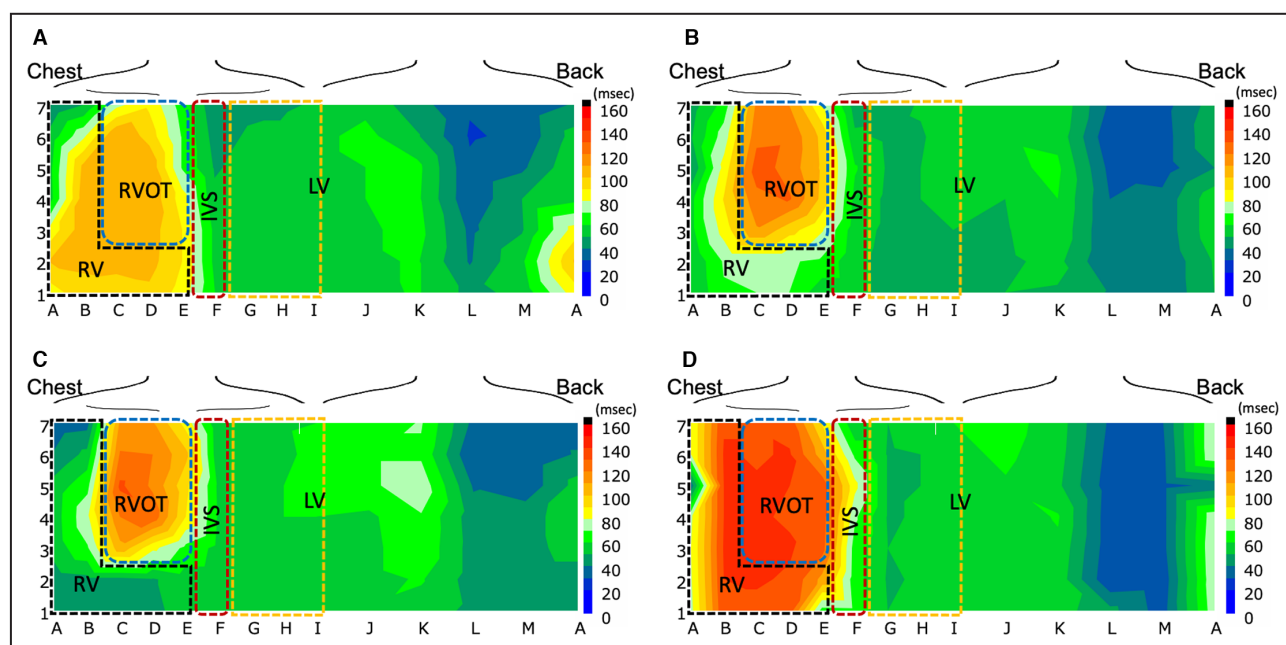


Figure 6. Average ventricular activation time map in each group.

We calculated the mean ventricular activation times of each unipolar lead in the control group, overall Brugada syndrome (BrS) group, BrS group without the proximal right bundle-branch block (RBBB) pattern, and BrS group with the proximal RBBB pattern. Then we created an isochronal map to evaluate the difference in the right ventricular (RV) activation pattern among these groups. **A**, Control group. **B**, BrS group (overall). **C**, BrS group with different RV activation pattern (Cases 1–7). **D**, BrS group with proximal RBBB pattern (Cases 8–11). In contrast to the control group, RV activation propagated faster in the inferior-lateral RV visually in the BrS group. This difference in RV activation was more obvious in the BrS group without the proximal RBBB pattern. In the BrS group with the proximal RBBB pattern, the entire RV activation was more delayed compared with that in the control group. Black dot square shows inferolateral RV, blue dot square shows RVOT and mild RV, brown dot square shows intraventricular septum, and yellow dot square shows left ventricle. IVS indicates intraventricular septum; LV, left ventricle; RV, right ventricle; and RVOT, right ventricular outflow tract.

We compared the BSM and VAT maps before and after CRBBB in BrS Case 2, in which incomplete RBBB developed CRBBB spontaneously (Figure 9). Before CRBBB, activation in the RV started from the mid RV to the RVOT with delayed conduction. After the development of CRBBB, the area with significantly delayed conduction was enlarged in the RV, but conduction in the inferolateral RV did not seem to be disturbed.

Four patients in the BrS group experienced VF recurrence. Three of those patients (Cases 1–3) exhibited the RV activation pattern without proximal RBBB, and 1 patient (Case 9) exhibited the same pattern with proximal RBBB. In Case 2, frequent appropriate therapies by an implantable cardioverter-defibrillator were performed after the development of CRBBB.

Difference of the QTc Interval and QTc Heterogeneity in the RVOT

Figure 10 shows QTc interval maps according to the mean QTc interval for each patient. These maps show that longer QTc intervals were observed in the RVOT, mid RV, and septum, and a shorter QTc interval was observed in the inferolateral and posterior LV in both

the BrS and control groups. However, there was a greater gradient in the QTc interval in the RV in the BrS group. Statistical analysis did not reveal significant QTc heterogeneity within the RVOT between the BrS and control groups (40.6 ± 24.2 ms versus 25.5 ± 9.2 ms, $P=0.081$). There was no obvious difference in the QTc interval map between the BrS groups with and without proximal RBBB (Figures 10C and 10D). The QTc interval maps of all patients and controls are shown in Figures S2 and S3.

Difference in Unipolar Electrocardiograms on BSM

We reviewed unipolar electrocardiograms of the anterolateral inferior RV (C1-2, D1-2) where VAT was visually faster in patients with BrS, except for the lateral RV. Figure 11 shows the typical and atypical morphologies of the unipolar leads of this area in each RV activation pattern. Figure 11A shows an example of a typical proximal RBBB in the control group (Case 3), and 4/4 leads exhibited rsR', rSR', or rR' morphology, which was ordinarily observed in the V1 lead of a patient with CRBBB (Figure 11A). In the BrS group without the

Table 2. Comparisons of VAT in Each Divided Area of Anterior Ventricle Between BrS and Control Groups

VAT, mean (SD)	BrS group	BrS group without the proximal RBBB pattern	Control group	P value for mixed effect model (BrS vs control)	P value for mixed effect model (BrS without the proximal RBBB pattern vs control)
Number of leads, overall	N=649	N=413	N=472		
VAT, ms	79.3 (40.8)	68.3 (35.6)	74.6 (30.2)		
Log-transformed VAT	4.25 (0.50)	4.11 (0.47)	4.23 (0.42)	0.83	0.20
Number of leads, inferior and lateral RV	N=198	N=126	N=144		
VAT, ms	76.4 (46.4)	52.7 (30.3)	89.1 (29.9)		
Log-transformed VAT	4.15 (0.62)	3.85 (0.46)	4.41 (0.45)	0.20	0.003
Number of leads, RVOT and mid RV	N=165	N=105	N=120		
VAT, ms	116.3 (39.5)	106.0 (42.8)	92.7 (32.3)		
Log-transformed VAT	4.67 (0.47)	4.55 (0.52)	4.44 (0.46)	0.115	0.49
Number of leads, septum	N=77	N=49	N=56		
VAT, ms	63.5 (25.1)	55.9 (10.0)	52.1 (13.4)		
Log-transformed VAT	4.10 (0.31)	4.01 (0.18)	3.93 (0.22)	0.08	0.31
Number of leads, LV	N=209	N=133	N=152		
VAT, ms	58.8 (8.4)	57.8 (8.8)	54.8 (7.8)		
Log-transformed VAT	4.06 (0.15)	4.04 (0.16)	3.99 (0.15)	0.20	0.42

Values are given as mean VAT, ms (SD) and mean VAT (SD) in log scale. N indicates the number of the concerned leads in each divided area. BrS indicates Brugada syndrome; LV, left ventricle; RBBB, right bundle-branch block; RV, right ventricle; RVOT, right ventricular outflow tract; SD, standard deviation; VAT, ventricular activation time.

proximal RBBB pattern, no lead (0/4) showed typical CRBBB morphology (Case 5, [Figure 11B](#)), whereas all leads (4/4) showed typical CRBBB morphology in the BrS group with the proximal RBBB pattern (Case 10, [Figure 11C](#)). Although QRS morphology in V1 and V2 leads exhibited typical CRBBB morphology on 12-lead ECG, QRS morphology in the anterior–inferior leads (C1-2, D1-2) was different in the BrS group without the proximal RBBB pattern. The typical CRBBB morphology in these leads in the BrS group without the proximal RBBB pattern was significantly less frequent than in the control group ($29.3 \pm 48.3\%$ versus $84.4 \pm 22.9\%$, $P=0.0128$), whereas that in the BrS group with the proximal RBBB pattern was not significantly less frequent ($52.7 \pm 50\%$ versus $84.4 \pm 22.9\%$, $P=0.116$).

DISCUSSION

New Observation

The results of this BSM analysis showed that the mechanism underlying the development of CRBBB in patients with BrS consisted of 2 RV activation patterns. One RV activation pattern was similar to the proximal RBBB pattern, and the other pattern was intact RBB conduction with a significant conduction delay around the RVOT. The latter pattern showed intact inferior and lateral RV activations. It is also noteworthy that the difference in the RV activation pattern in patients

with BrS with CRBBB might be emphasized by comparing patients in whom the proximal RBB was definitively disturbed. A localized activation delay around the RVOT could also result in CRBBB morphology in BrS. However, the number of patients was small, and it might be difficult to apply the results of the present study to all patients with BrS with CRBBB. The observation that control patients never showed a pattern of localized conduction delay in the RVOT area, while patients with BrS frequently had that pattern, might indicate that localized conduction delay is one of the common mechanisms of CRBBB in patients with BrS.

Activation Pattern in the RV

RBB typically takes an intramuscular course within the septum before it becomes more superficial at the base of the medial papillary muscle of the RV. The right bundle band directs the attachment of the moderator band, which extends to the anterior papillary muscle located at the apical third of the RV free wall. Purkinje fibers from the RBB subsequently activate the rest of the RV subendocardium.^{11,26,27} Epicardial RV activation usually expands radially from the base of the anterior papillary muscle to the pulmonary sulcus and posterobasal area, which are the latest activated areas in the RV.^{27,28} Previous studies demonstrated that RV activation in the usual CRBBB condition was markedly delayed in the entire RV, the epicardial breakthrough site

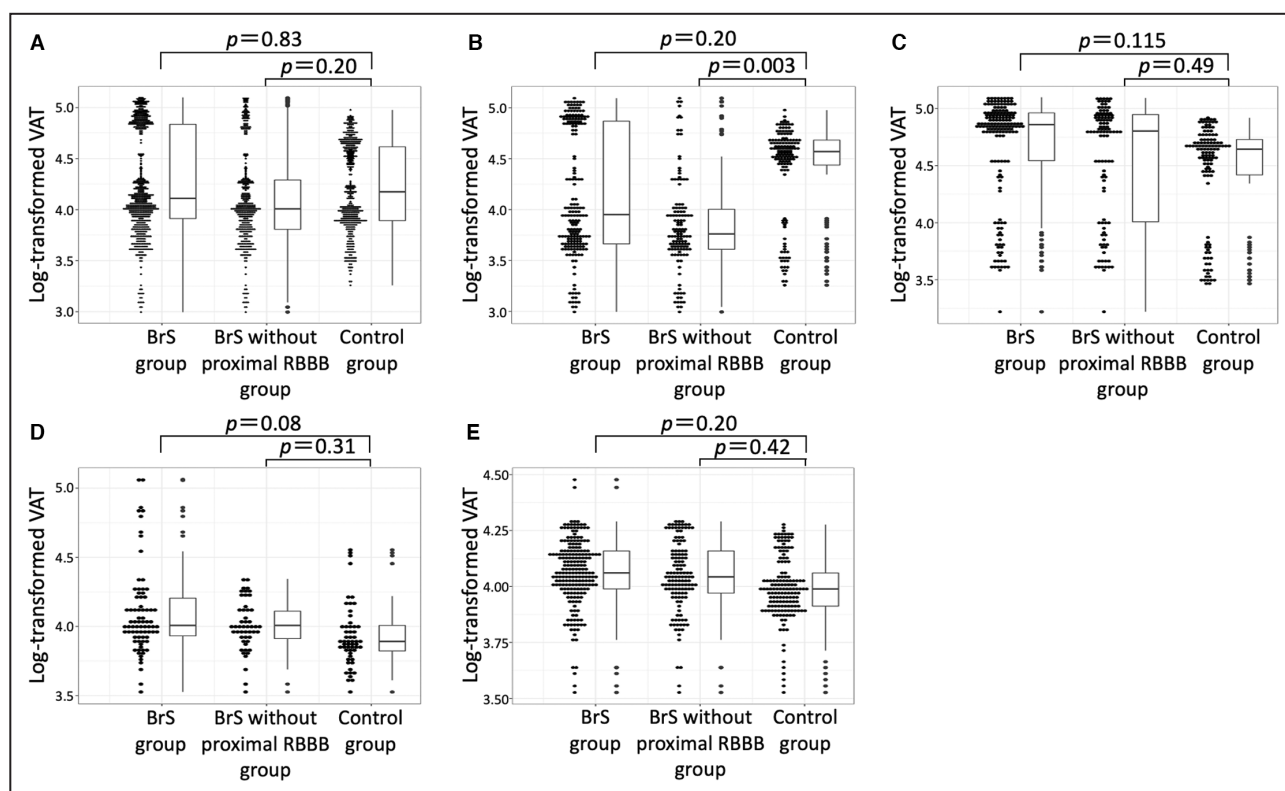


Figure 7. Comparisons of log-transformed ventricular activation time in each divided area of anterior ventricle between the Brugada syndrome and the control groups.

A, Log-transformed ventricular activation time (VAT) in overall Brugada syndrome (BrS) patients, Patients with BrS without proximal right bundle-branch block (RBBB) and control. **B**, VAT in inferior and lateral right ventricle (RV). There was no significant difference in VAT between the overall BrS group and the control group. VAT at the inferior and lateral RV in the BrS group without the proximal RBBB pattern was significantly shorter than that in the control group. VAT right ventricular outflow tract and mid RV (**C**), intraventricular septum (**D**), and left ventricle (**E**) were not different between overall BrS patients and control group, and between BrS without proximal RBBB and control.

in the RV was absent,^{28,29} and conduction delay was observed in the septum. In this BSM study, the RV activation pattern in the control group, in which CRBBB was developed by bump at the main RBB, was the

same as that in patients without obvious heart disease (Figure S1). From the observations in previous studies and the present study, conduction block at the trunk of the RBB is considered to be an ordinary mechanism of

Table 3. Comparisons of the Latest VAT in Each Divided Area of Ventricle Between BrS and Control Groups

Latest VAT, mean (SD)	Control group (n=8)	BrS group (n=11)	P value
Inferior and lateral RV			
Latest VAT, ms	112.8 (17.0)	109.5 (47.2)	
Log-transformed latest VAT	4.72 (0.14)	4.59 (0.52)	0.60
RVOT and mid RV			
Latest VAT, ms	113.6 (15.6)	138.8 (20.9)	
Log-transformed latest VAT	4.72 (0.14)	4.92 (0.16)	0.012
Septum			
Latest VAT, ms	63.4 (18.0)	82.5 (34.5)	
Log-transformed latest VAT	4.12 (0.26)	4.35 (0.37)	0.09
LV			
Latest VAT, ms	61.1 (7.5)	68.0 (8.6)	
Log-transformed latest VAT	4.11 (0.12)	4.21 (0.12)	0.08

Values are given as the mean latest VAT, ms (SD) and mean latest VAT (SD) in log scale. n indicates the number of the included patients of each group. BrS indicates Brugada syndrome; LV, left ventricle; RV, right ventricle; RVOT, right ventricular outflow tract; and VAT, ventricular activation time.

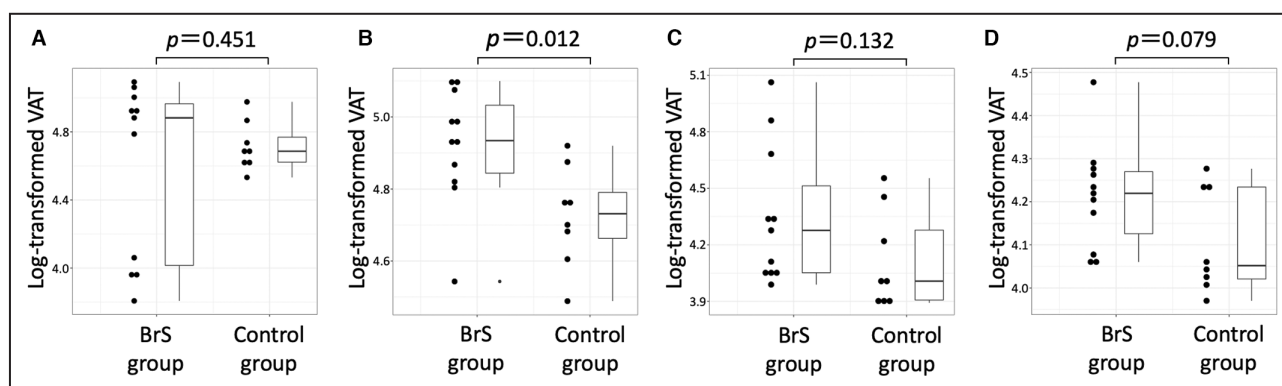


Figure 8. Comparisons of the latest ventricular activation time in each divided area of ventricle between the Brugada syndrome and the control groups.

Comparison of the latest ventricular activation time (VAT) in each area (A), inferior and lateral right ventricle (RV), (B), right ventricular outflow tract (RVOT) and mid RV, (C), intraventricular septum, and (D), left ventricle. The latest VAT in the RVOT and mid RV in the Brugada syndrome (BrS) group was significantly longer than that in the control group. The latest VATs in other area in the BrS were not significantly different.

CRBBB. Our BSM study also revealed 2 RV activation patterns in the BrS group that were similar and dissimilar to the proximal RBBB pattern. A previous study showed that some patients with BrS had conduction disturbances through their conduction system in the

RV.³⁰ Thus, patients in the BrS group with the proximal RBBB pattern might have had a disturbed site at the proximal RBB and developed a CRBBB pattern similar to that of patients in the control group. In contrast, there was a significant conduction disturbance around

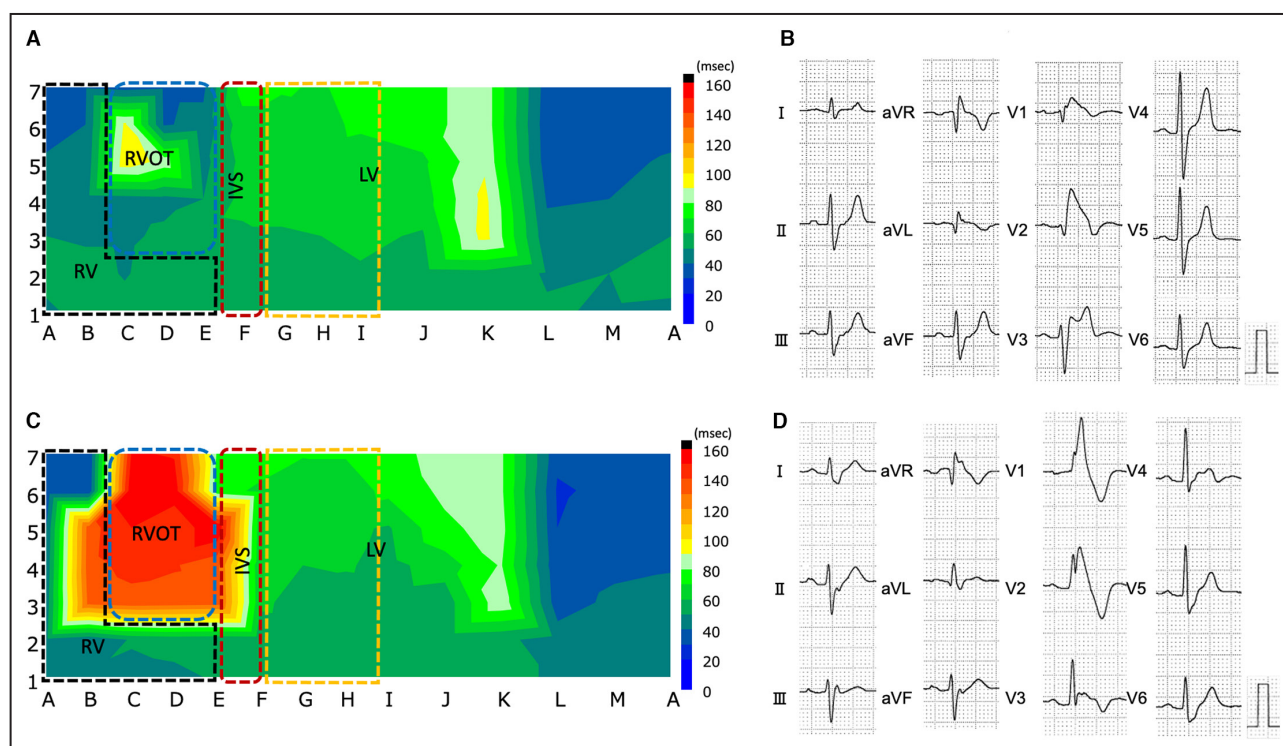


Figure 9. Ventricular activation time maps before and after development of complete right bundle-branch block in Brugada syndrome group Case 2.

The maps show isochronal maps of ventricular activation time before (A) and after (B) development of complete right bundle-branch block (CRBBB) in Brugada syndrome Case 2. The area of significant delayed conduction was larger after CRBBB than before CRBBB. However, activation in the inferolateral region in the right ventricle did not seem to be different before and after CRBBB (C). Black dot square shows inferolateral RV, blue dot square shows RVOT and mild RV, brown dot square shows intraventricular septum, and yellow dot square shows left ventricle. IVS indicates intraventricular septum; LV, left ventricle; RV, right ventricle; and RVOT, right ventricular outflow tract.

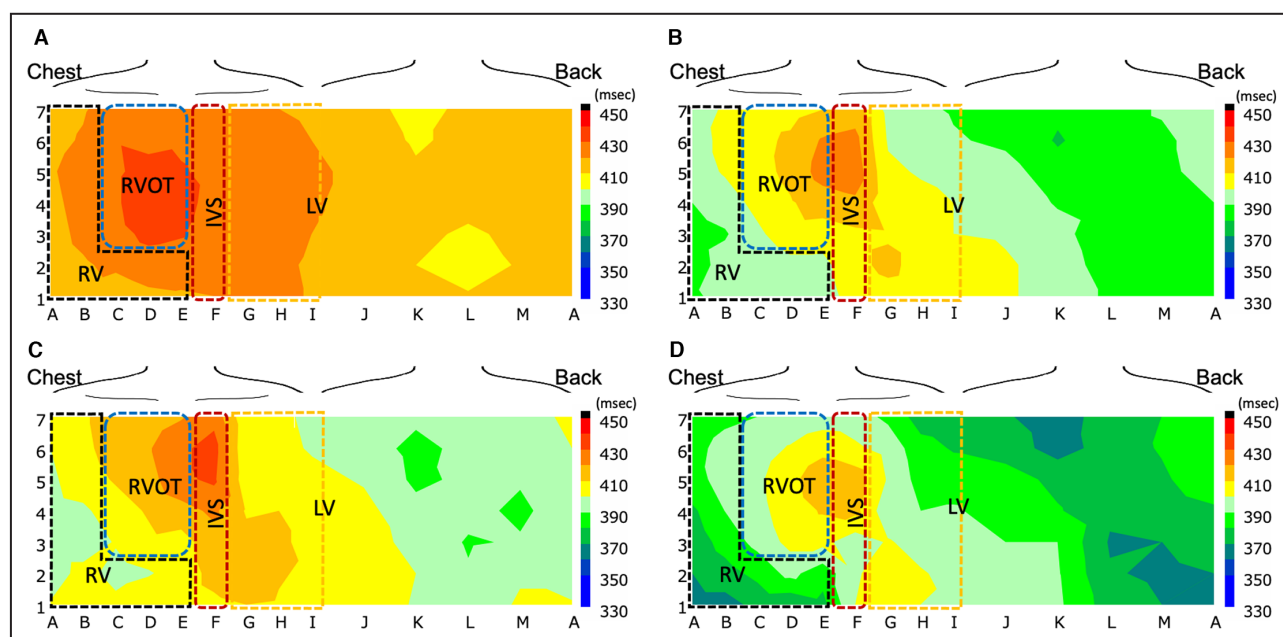


Figure 10. Average QTc interval map in each group.

A, Control group. **B**, Brugada syndrome (BrS) group (overall). **C**, BrS group without proximal right bundle-branch block (RBBB) pattern (Cases 1–7). **D**, BrS group with proximal RBBB pattern (Cases 8–11). Longer QTc interval was observed in right ventricular outflow tract (RVOT), mid RV and septum, and shorter QTc interval was observed in inferolateral RV and posterior left ventricle (LV) in both the BrS and control groups. There was no QTc interval heterogeneity within RVOT area in both of the groups. There was no obvious QTc interval distribution between the BrS group with and without proximal RBBB. Black dot square shows inferolateral RV, blue dot square shows RVOT and mild RV, brown dot square shows intraventricular septum, and yellow dot square shows left ventricle. IVS indicates intraventricular septum; and RV, right ventricle.

the RVOT in patients with BrS without a proximal RBBB pattern. Zhang et al reported the difference in RV activation patterns between patients with BrS and patients with usual RBBB by analyzing ECG imagings.³¹ Their study showed that RV activation started from epicardial breakthrough at the anterior paraseptal site and propagated to the RVOT with conduction delay, whereas the inferior and lateral RV were excited radially from the epicardial breakthrough without conduction delay. These areas were excited faster in patients with BrS with RBBB than in patients without BrS with RBBB. Because the rSR' pattern was often observed in leads V1 and V2, which were placed in higher intercostal spaces,³² their study did not describe whether the CRBBB pattern was observed at standard intercostal leads in the patients with BrS. In the present study, which focused on patients with BrS with CRBBB at standard intercostal leads, the VAT was faster in the inferior and lateral RV than in the septum in patients in the BrS group without the proximal RBBB pattern. This suggested that conduction up to the distal RBB might be maintained, and activation propagated normally in the inferior and lateral RV, as was observed in the previous study. These different activation patterns might result in different QRS morphologies in the anterior-inferior unipolar leads in the BSM, which represent the

inferior RV. In patients in the control and BrS groups with the proximal RBBB pattern, most of the unipolar leads in this area showed a typical CRBBB morphology. In contrast, a significantly smaller number of leads in this area exhibited typical CRBBB in patients in the BrS group without the proximal RBBB.

Different Sources of Conduction Delay

Although CRBBB is defined by ECG findings, different blocked sites of the conduction system in the RV can exhibit similar QRS morphologies. Patients without obvious heart disease had conduction block at the main trunk of the RBB, whereas patients with organic heart disease could have CRBBB patterns at various levels along with the RBB-to-Purkinje connection. Horowitz et al reported that RBBB could be caused by 3 potential levels of delayed conduction in the RV during intraoperative endocardial and epicardial mapping in patients with congenital heart disease: proximal, distal, and terminal RBBB.¹⁵ In the proximal RBBB, RV activation starts via transeptal spread from the LV and then propagates in the mid and apical RV septum, RV anterior free wall, and RVOT. In contrast, activation along the His bundle and RBB remained normal up to the Purkinje junction in the terminal RBBB. Hence,

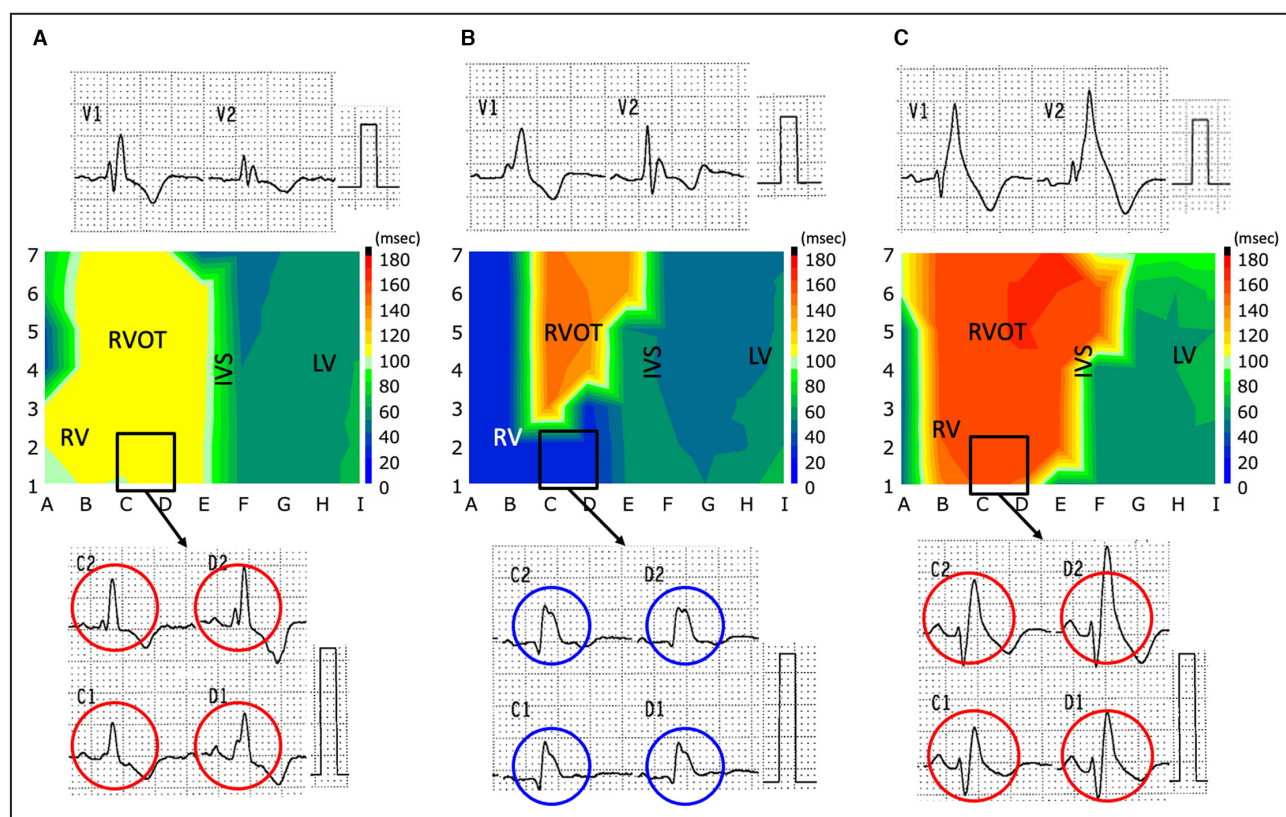


Figure 11. Comparison of QRS morphologies in anterior inferior unipolar leads in each group.

Investigation of whether 4 unipolar leads (C1-2, D1-2) presented with rsR', rSR', or rR' morphology. The red circle indicates typical complete right bundle-branch block (CRBBB) morphology, and the blue circle indicates atypical CRBBB morphology. (A) 4/4 unipolar leads presented with typical CRBBB morphology, as was observed in many cases in the control group (control Case 1). (B) 0/4 unipolar leads presented with typical CRBBB morphology in the Brugada syndrome (BrS) group without the proximal right bundle-branch block (RBBB) pattern (BrS Case 5). (C) 4/4 unipolar leads presented with typical CRBBB morphology in the BrS group with the proximal RBBB pattern (BrS Case 10). IVS indicates intraventricular septum; LV, left ventricle; RV, right ventricle; and RVOT, right ventricular outflow tract.

RV activation of the midanterior wall was unchanged from normal, and only RVOT activation was delayed, in contrast to proximal RBBB. The authors suggested that terminal RBBB is likely to be associated with disturbance of the distal conduction system of the RBB, Purkinje fibers, or the muscle itself in patients with congenital heart disease. Although RV activation in the distal RBBB resembles that in the terminal RBBB, the level of block was suggested to be a moderator band. In the present study, RV activation in patients in the BrS group without the proximal RBBB pattern was likely to be consistent with the terminal RBBB in the abovementioned classification. Recent studies have revealed structural abnormality in the epicardium and subepicardium and electrical abnormality in the RVOT in patients with BrS.^{5,33,34} These abnormalities might have yielded the RV activation pattern observed in patients in the BrS group without a proximal RBBB. In addition, RV activation did not start from the mid-paraseptal area in the RV of patients in the BrS group without the proximal RBBB. In previous studies, the site of epicardial breakthrough in the RV was observed

in the midanterior paraseptal area in patients without the proximal RBBB.^{35–37} This observation might indicate that conduction disturbance was located not only in the RVOT but also in the area surrounding the RVOT, including the area of epicardial breakthrough in patients with BrS with terminal CRBBB. Although there could be some conduction delay through the conduction system in the RV,³⁰ larger epicardial depolarization abnormalities around the RVOT might contribute to CRBBB morphology in patients with BrS without proximal RBBB. This speculation might be confirmed by the high rate of fatal arrhythmic events in patients with BrS with CRBBB.¹⁰ Indeed, 3 of 4 patients without proximal CRBBB who experienced VF had frequent VF episodes and implantable cardioverter-defibrillator discharges. Average VAT maps showed that entire RV activation was more delayed in patients in the BrS group with the proximal RBBB pattern than in patients in the control group. It is conceivable that the existence of depolarization abnormality in the RV also yielded a more delayed conduction in patients with BrS with proximal RBBB than in patients in the control group

with proximal RBBB. Previously, we reported activation patterns during VF in patients with BrS, and foci and conduction abnormality in the RVOT seem to be important for the initiation of VF.²³

The QTc interval map showed a longer QTc area from the RVOT to the intraventricular septum in both BrS and control patients, and QTc interval heterogeneity within the RVOT was not observed in patients with BrS. A previous study reported a steep QT gradient in the RVOT area in a patient with BrS when premature ventricular contractions occurred from the RVOT after administration of sodium channel blocker.¹⁷ The BSM was recorded in a stable condition without sodium channel blocker in the present study; thus the repolarization condition might not have been irritable for arrhythmogenicity.

Limitations

In addition to the retrospective observational study design, our study had several limitations. First, the number of patients in this study was small, and the findings should therefore be interpreted as exploratory in nature. Second, the leads in BSM did not always accurately represent the same area of the ventricle in each patient. Although we assumed a correlation between the body surface area and each ventricular region based on previous BSM studies,^{23,24} unipolar leads could reflect slightly different regions because of the differences in the position of each patient's heart and body constitution. Finally, we calculated the VAT by the peak negative dV/dT of the QRS complex in each unipolar ECG on the BSM. The VAT did not accurately reflect the activation time of the closest epicardium because the unipolar ECG on the BSM should consist of a summation of the activations from the endocardium to epicardium, and intraventricular septum.

CONCLUSIONS

This study revealed the activation pattern in the RV and the source of delayed conduction in patients with BrS with CRBBB. We confirmed a significant conduction delay around the RVOT in patients with BrS with CRBBB. This RV activation pattern was different from that observed in the usual CRBBB, which had delayed conduction at the proximal RBB. Extended depolarization abnormality around the RVOT could indicate CRBBB morphology in patients with BrS.

ARTICLE INFORMATION

Received November 2, 2022; accepted April 6, 2023.

Affiliations

Department of Cardiovascular Medicine (Y.M., K.E., T. Mizuno, T. Masuda, A.U., S.A., M.M., S.K., K. Nakagawa, K. Nakamura, H.I.) and Department

of Cardiovascular Therapeutics (H.M., N.N.), Okayama University Graduate School of Medicine, Dentistry, and Pharmaceutical Sciences, Okayama, Japan; Department of Cardiovascular Medicine, Fukuyama City Hospital, Hiroshima, Japan (Y.M.); and Department of Epidemiology, Johns Hopkins Bloomberg School of Public Health, Baltimore, MD (K.E.).

Sources of Funding

This study was supported by Japan Society for the Promotion of Science KAKENHI (21K08028 to H.M.).

Disclosures

Dr Nobuhiro Nishii and Dr Hiroshi Morita are affiliated with the endowed department by Japan Medtronic Inc. The remaining authors have no disclosures to report.

Supplemental Material

Figures S1–S3

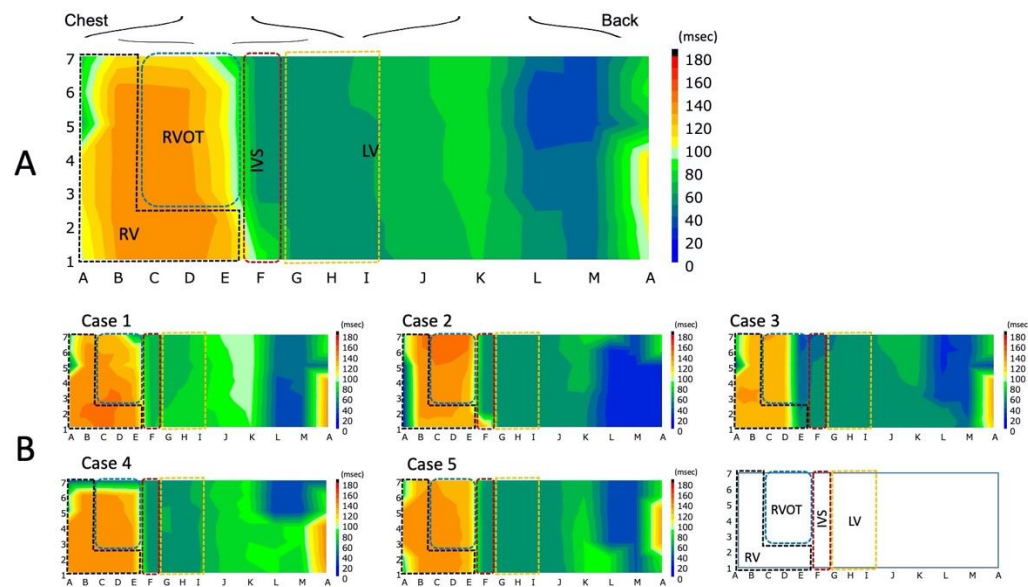
REFERENCES

1. Priori SG, Wilde AA, Horie M, Cho Y, Behr ER, Berul C, Blom N, Brugada J, Chiang CE, Huikuri H, et al. HRS/EHRA/APHRS expert consensus statement on the diagnosis and management of patients with inherited primary arrhythmia syndromes: document endorsed by HRS, EHRA, and APHRS in May 2013 and by ACCF, AHA, PACES, and AEPC in June 2013. *Heart Rhythm*. 2013;10:1932–1963. doi: 10.1016/j.hrthm.2013.05.014
2. Antzelevitch C, Brugada P, Brugada J, Brugada R, Towbin JA, Nademanee K. Brugada syndrome: 1992–2002. *J Am Coll Cardiol*. 2003;41:1665–1671. doi: 10.1016/S0735-1097(03)00310-3
3. Patocskaï B, Yoon N, Antzelevitch C. Mechanisms underlying epicardial radiofrequency ablation to suppress arrhythmogenesis in experimental models of Brugada syndrome. *JACC Clin Electrophysiol*. 2017;3:353–363. doi: 10.1016/j.jacep.2016.10.011
4. Nagase S, Kusano KF, Morita H, Fujimoto Y, Kakishita M, Makamura K, Emori T, Matsubara H, Tohru O. Epicardial electrogram of the right ventricular outflow tract in patients with the Brugada syndrome. *J Am Coll Cardiol*. 2002;39:1992–1995. doi: 10.1016/S0735-1097(02)01888-0
5. Nademanee K, Raju H, de Noronha SV, Papadakis M, Robinson L, Rothery S, Makita N, Kowase S, Boonmee N, Vitayakritsirikul V, et al. Fibrosis, connexin-43, and conduction abnormalities in the Brugada syndrome. *J Am Coll Cardiol*. 2015;66:1976–1986. doi: 10.1016/j.jacc.2015.08.862
6. Meregalli PG, Wilde AAM, Tan HL. Pathophysiological mechanisms of Brugada syndrome: depolarization disorder, repolarization disorder, or more? *Cardiovasc Res*. 2005;67:367–378. doi: 10.1016/j.cardiores.2005.03.005
7. Nademanee K, Veerakul G, Chandanamatha P, Chaothawee L, Ariyachaipanich A, Jirasirojanakorn K, Likittanasombat K, Bhuripanyo K, Ngarmukos T. Prevention of ventricular fibrillation episodes in Brugada syndrome by catheter ablation over the anterior right ventricular outflow tract epicardium. *Circulation*. 2011;123:1270–1279. doi: 10.1161/CIRCULATIONAHA.110.972612
8. Pappone C, Brugada J, Vicedomini G, Ciccone G, Manguso F, Saviano M, Vitale R, Cuko A, Giannelli L, Calovic Z, et al. Electrical substrate elimination in 135 consecutive patients with Brugada syndrome. *Circ Arrhythm Electrophysiol*. 2017;10:e005053.
9. Nademanee K, Hocini M, Haissaguerre M. Epicardial substrate ablation for Brugada syndrome. *Heart Rhythm*. 2017;14:457–461. doi: 10.1016/j.hrthm.2016.12.001
10. Morita H, Watanabe A, Kawada S, Miyamoto M, Morimoto Y, Nakagawa K, Nishii N, Nakamura K, Ito H. Identification of electrocardiographic risk markers for the initial and recurrent episodes of ventricular fibrillation in patients with Brugada syndrome. *J Cardiovasc Electrophysiol*. 2018;29:107–114. doi: 10.1111/jce.13349
11. Josephson ME, ed. *Josephson's Clinical Cardiac Electrophysiology: Techniques and Interpretations*. 5th ed. Wolters Kluwer Health; 2016.
12. Tan NY, Witt CM, Oh JK, Cha YM. Left bundle branch block: current and future perspectives. *Circ Arrhythm Electrophysiol*. 2020;13:e008239. doi: 10.1161/CIRCEP.119.008239
13. Upadhyay GA, Cherian T, Shatz DY, Beaser AD, Aziz Z, Ozcan C, Broman MT, Nayak HM, Tung R. Intracardiac delineation of septal conduction in

- left bundle-branch block patterns. *Circulation*. 2019;139:1876–1888. doi: 10.1161/CIRCULATIONAHA.118.038648
14. Lev M, Unger PN, Lesser ME, Pick A. Pathology of the conduction system in acquired heart disease. Complete right bundle branch block. *Am Heart J*. 1961;61:593–614. doi: 10.1016/0002-8703(61)90630-5
 15. Horowitz LN, Alexandr JA, Edmunds LH. Postoperative RBBB identification of three levels of block. *Circulation*. 1980;62:327–328.
 16. Surawicz B, Childers R, Deal BJ, Gettes LS, Bailey JJ, Gorgels A, Hancock EW, Josephson M, Kligfield P, Kors JA, et al. AHA/ACCF/HRS recommendations for the standardization and interpretation of the electrocardiogram: part III: intraventricular conduction disturbances: a scientific statement from the American Heart Association Electrocardiography and Arrhythmias Committee, Council on Clinical Cardiology; the American College of Cardiology Foundation; and the Heart Rhythm Society. Endorsed by the International Society for Computerized Electrocardiology. *Circulation*. 2009;119:e235–e240. doi: 10.1161/CIRCULATIONAHA.108.191095
 17. Morita H, Zipes DP, Kusano KF, Nagase S, Nakamura K, Morita ST, Ohe T, Wu J. Repolarization heterogeneity in the right ventricular outflow tract: correlation with ventricular arrhythmias in Brugada patients and in an in vitro canine Brugada model. *Heart Rhythm*. 2008;5:725–733. doi: 10.1016/j.hrthm.2008.02.028
 18. Morita H, Kusano KF, Miura D, Nagase S, Nakamura K, Morita ST, Ohe T, Zipes DP, Wu J. Fragmented QRS as a marker of conduction abnormality and a predictor of prognosis of Brugada syndrome. *Circulation*. 2008;118:1697–1704. doi: 10.1161/CIRCULATIONAHA.108.770917
 19. Das MK, Suradi H, Maskoun W, Michael MA, Shen C, Peng J, Dandamudi G, Mahenthiran J. Fragmented wide QRS on a 12-lead ECG: a sign of myocardial scar and poor prognosis. *Circ Arrhythm Electrophysiol*. 2008;1:258–268. doi: 10.1161/CIRCEP.107.763284
 20. Ikeda T, Sakurada H, Sakabe K, Sakata T, Takami M, Tezuka N, Nakae T, Noro M, Enjoji Y, Tejima T, et al. Assessment of noninvasive markers in identifying patients at risk in the Brugada syndrome: insight into risk stratification. *J Am Coll Cardiol*. 2001;37:1628–1634. doi: 10.1016/S0735-1097(01)01197-4
 21. Babai Bigi MA, Aslani A, Shahrzad S. aVR sign as a risk factor for life-threatening arrhythmic events in patients with Brugada syndrome. *Heart Rhythm*. 2007;4:1009–1012. doi: 10.1016/j.hrthm.2007.04.017
 22. Calo L, Giustetto C, Martino A, Sciarra L, Cerrato N, Marziali M, Rauzino J, Carlino G, de Ruvo E, Guerra F, et al. A new electrocardiographic marker of sudden death in Brugada syndrome: the S-wave in lead I. *J Am Coll Cardiol*. 2016;67:1427–1440. doi: 10.1016/j.jacc.2016.01.024
 23. Ueoka A, Morita H, Watanabe A, Nakagawa K, Nishii N, Nagase S, Ohe T, Ito H. Activation pattern of the polymorphic ventricular tachycardia and ventricular fibrillation on body surface mapping in patients with Brugada syndrome. *Circ J*. 2016;80:1734–1743. doi: 10.1253/circj.CJ-16-0124
 24. Kamakura S, Shimizu W, Matsuo K, Taguchi A, Suyama K, Kurita T, Aihara N, Ohe T, Shimomura K. Localization of optimal ablation site of idiopathic ventricular tachycardia from right and left ventricular outflow tract by body surface ECG. *Circulation*. 1998;98:1525–1533. doi: 10.1161/01.CIR.98.15.1525
 25. Yamaki M, Ikeda K, Kubota I, Nakamura K, Hanashima K, Tsuike K, Yasui S. Improved diagnostic performance on the severity of left ventricular hypertrophy with body surface mapping. *Circulation*. 1989;79:312–323. doi: 10.1161/01.CIR.79.2.312
 26. Padala SK, Cabrera JA, Ellenbogen KA. Anatomy of the cardiac conduction system. *Pacing Clin Electrophysiol*. 2021;44:15–25. doi: 10.1111/pace.14107
 27. Durrer D, van Dam RT, Freud GE, Janse MJ, Meijler FL, Arzbaecher RC. Total excitation of the isolated human heart. *Circulation*. 1970;1970:899–912. doi: 10.1161/01.CIR.41.6.899
 28. Kawasumi M, Iwa T. Spread of the epicardial excitation in RBBB pattern. *Jpn Circ J*. 1978;42:1041–1056. doi: 10.1253/jcj.42.1041
 29. Duchateau J, Sacher F, Pambrun T, Derval N, Chamorro-Servent J, Denis A, Ploux S, Hocini M, Jais P, Bernus O, et al. Performance and limitations of noninvasive cardiac activation mapping. *Heart Rhythm*. 2019;16:435–442. doi: 10.1016/j.hrthm.2018.10.010
 30. Maury P, Rollin A, Sacher F, Gourraud JB, Raczká F, Pasquie JL, Duparc A, Mondoly P, Cardin C, Delay M, et al. Prevalence and prognostic role of various conduction disturbances in patients with the Brugada syndrome. *Am J Cardiol*. 2013;112:1384–1389. doi: 10.1016/j.amjcard.2013.06.033
 31. Zhang J, Sacher F, Hoffmayer K, O'Hara T, Strom M, Cuculich P, Silva J, Cooper D, Faddis M, Hocini M, et al. Cardiac electrophysiological substrate underlying the ECG phenotype and electrogram abnormalities in Brugada syndrome patients. *Circulation*. 2015;131:1950–1959. doi: 10.1161/CIRCULATIONAHA.114.013698
 32. Baranchuk A, Enriquez A, Garcia-Niebla J, Bayes-Genis A, Villuendas R, Bayes de Luna A. Differential diagnosis of rS_r' pattern in leads V1–V2. Comprehensive review and proposed algorithm. *Ann Noninvasive Electrocardiol*. 2015;20:7–17. doi: 10.1111/anec.12241
 33. Ten Sande JN, Coronel R, Conrath CE, Driessen AH, de Groot JR, Tan HL, Nademanee K, Wilde AA, de Bakker JM, van Dessel PF. ST-segment elevation and fractionated electrograms in Brugada syndrome patients arise from the same structurally abnormal subepicardial RVOT area but have a different mechanism. *Circ Arrhythm Electrophysiol*. 2015;8:1382–1392. doi: 10.1161/CIRCEP.115.003366
 34. Nademanee K, Veerakul G, Nogami A, Lou Q, Hocini M, Coronel R, Behr ER, Wilde A, Boukens BJ, Haissaguerre M. Mechanism of the effects of sodium channel blockade on the arrhythmogenic substrate of Brugada syndrome. *Heart Rhythm*. 2022;19:407–416. doi: 10.1016/j.hrthm.2021.10.031
 35. Medvegy M, Duray G, Pintér A, Prédá I. Body surface potential mapping: historical background, present possibilities, diagnostic challenges. *Ann Noninvasive Electrocardiol*. 2002;7:139–151. doi: 10.1111/j.1542-474X.2002.tb00155.x
 36. Sugeno Y. Interpretation of the body surface isopotential maps of patients with right bundle branch block. *Jpn Heart J*. 1978;19:12–27. doi: 10.1536/ihj.19.12
 37. Yamada K. Body surface isopotential map. Past, present and future. *Jpn Circ J*. 1981;45:1–14. doi: 10.1253/jcj.45.1

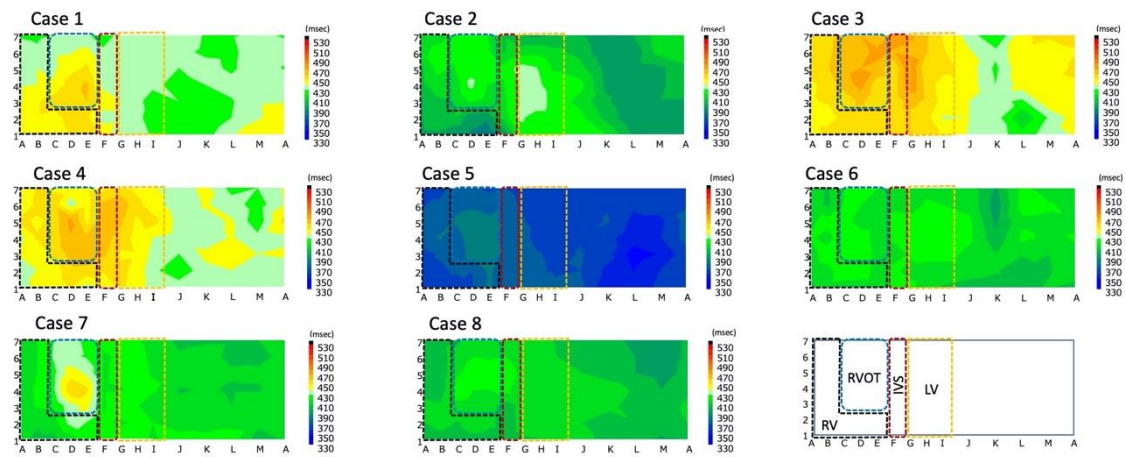
SUPPLEMENTAL MATERIAL

Figure S1. Ventricular activation maps of the CRBBB without obvious heart disease.



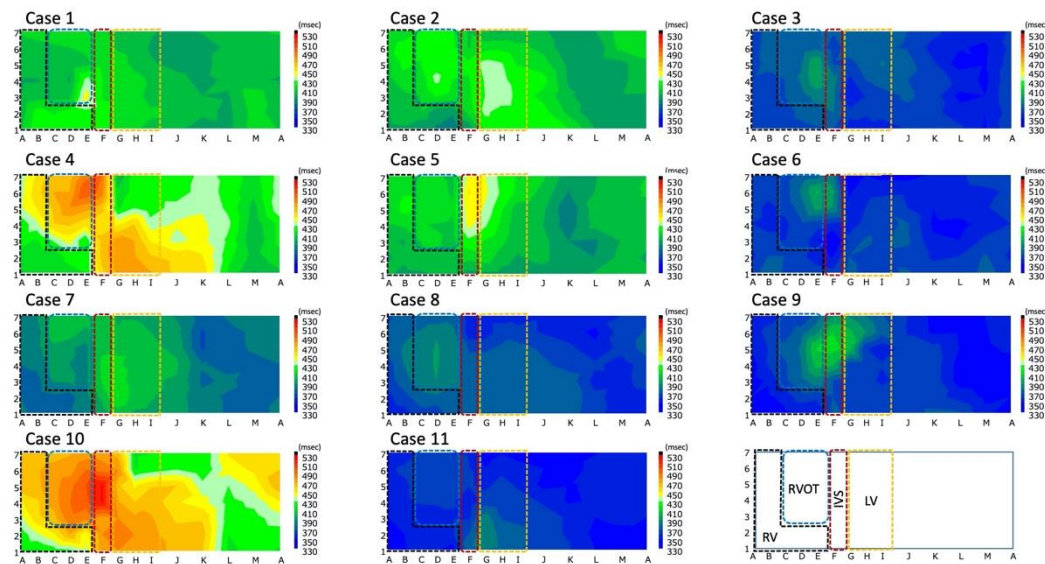
A. Average ventricular activation (VAT) map in patients with complete right bundle branch block (CRBBB) not having obvious heart disease. B. These figures exhibit the VAT maps of 5 patients with CRBBB who did not have obvious heart disease. These VAT maps showed entire right ventricular (RV) delay in these patients and the pattern was same as that of proximal RBBB. Black dot square shows inferolateral RV, blue dot square shows RVOT and mild RV, brown dot square shows intraventricular septum, yellow dot square shows left ventricle. IVS: intraventricular septum, LV: left ventricle, RV: right ventricle, RVOT: right ventricular outflow tract

Figure S2. QTc interval map in the control group.



Isochronal maps of QTc interval in control cases (Case 1–8). There was low gradient of QTc interval in overall ventricles. Black dot square shows inferolateral RV, blue dot square shows RVOT and mild RV, brown dot square shows intraventricular septum, yellow dot square shows left ventricle. IVS: intraventricular septum, LV: left ventricle, RV: right ventricle, RVOT: right ventricular outflow tract

Figure S3. QTc interval map in the control group.



Isochronal maps of QTc interval in Brugada syndrome (BrS) cases (Case 1–11).

There were more gradient of QTc interval around the right ventricular outflow tract (RVOT)/mid RV and septum in the BrS group than in the control group. There was no QTc interval heterogeneity within RVOT area. Black dot square shows inferolateral RV, blue dot square shows RVOT and mild RV, brown dot square shows intraventricular septum, yellow dot square shows left ventricle. IVS: intraventricular septum, LV: left ventricle, RV: right ventricle, RVOT: right ventricular outflow tract